



# Synthesis and biological evaluation of 2,4-disubstituted thiazole amide derivatives as anticancer agent

Zhi-Hua Zhang<sup>1</sup> · Hong-Mei Wu<sup>1</sup> · Sai-Nan Deng<sup>2</sup> · Rui-Xia Chai<sup>2</sup> · Muriira Cyrus Mwenda<sup>2</sup> · Yuan-Yuan Peng<sup>2</sup> · Dong Cai<sup>3</sup> · Yu Chen<sup>4</sup>

Received: 6 April 2018 / Accepted: 1 September 2018  
© Institute of Chemistry, Slovak Academy of Sciences 2018

## Abstract

A series of novel 2,4-disubstituted thiazole amide derivatives were synthesized, and their antiproliferative activities were tested. Some of these compounds displayed good antiproliferative activity, especially for HT29 cell. Among these compounds, compound **5b** inhibits A549, HeLa, HT29 and Karpas299 cells with IC<sub>50</sub> values of 8.64, 6.05, 0.63 and 13.87 μM, respectively. The western blot analysis and docking study provide important clues for further optimization of compound **5b** as a potential c-Met inhibitor.

**Keywords** Thiazole derivatives · Synthesis · Anticancer activity

## Introduction

2-Aminothiazole derivatives, especially 4-phenylthiazol-2-amines, have attracted interest over the last decades for their multiple biological activities (Alam et al. 2011; Siddiqui et al. 2007; Zhou et al. 2008), and many derivatives of 4-phenylthiazol-2-amine are well known as anticancer agents **1–2** (Fig. 1). The position of the substituents on the phenyl group and the type of the substituents on the 2-amino group are responsible for the variety of antiproliferative

activities (Bhat et al. 2013; Chang et al. 2012; El-Messery et al. 2012; Smith et al. 2012; Hassan et al. 2012).

Recently, we have discovered many compounds that possess anticancer activity, such as novel ALK inhibitors (Gennäs et al. 2011; Tu et al. 2016) **3** and **4** (Fig. 1). These active compounds are structurally similar to 4-phenylthiazol-2-amines and display discrete structural overlap with the 4-phenylthiazol-2-amine scaffold.

Crizotinib (PF-02341066), developed by Pfizer Inc., is a potent inhibitor of c-Met and ALK with IC<sub>50</sub> of 11 nM and 24 nM in cell-based assays, respectively (Cui et al. 2011). This compound was approved by the FDA in 2014 for patients with bladder cancer, non-Hodgkin's lymphoma, renal cell carcinoma and non-small cell lung cancer (NSCLC) (Wilson et al. 2014). However, crizotinib induced some adverse reactions, including vision disorder, nausea, diarrhea, vomiting, constipation, edema, elevated transaminases, and fatigue (Solomon 2014).

Inspired by the above-mentioned facts and in continuation of our research program on inhibitory activities of 4-phenylthiazol-2-amine derivatives, crizotinib was selected as a backbone for the development of novel 2,4-disubstituted thiazole amide derivatives (Fig. 2). Using a scaffold modification strategy, we employed a substituted 4-phenylthiazol-2-amine moiety instead of a substituted 3-(1*H*-pyrazol-4-yl) pyridine fragment of crizotinib. The 2-amino function of the 4-phenylthiazol-2-amine core was also acylated to produce the terminal 2-morpholinoacetamido fragment, whose

**Electronic supplementary material** The online version of this article (<https://doi.org/10.1007/s11696-018-0587-3>) contains supplementary material, which is available to authorized users.

✉ Dong Cai  
Caidong0804@163.com

✉ Yu Chen  
gzweishengwu@126.com

<sup>1</sup> School of Chemical and Environmental Engineering, Liaoning University of Technology, Jinzhou 121001, China

<sup>2</sup> College of Pharmacy, Jinzhou Medical University, Jinzhou 121001, China

<sup>3</sup> College of Basic Science, Jinzhou Medical University, Jinzhou 121001, China

<sup>4</sup> School of Life Science and Biopharmaceutics, Shenyang Pharmaceutical University, Shenyang 110016, China

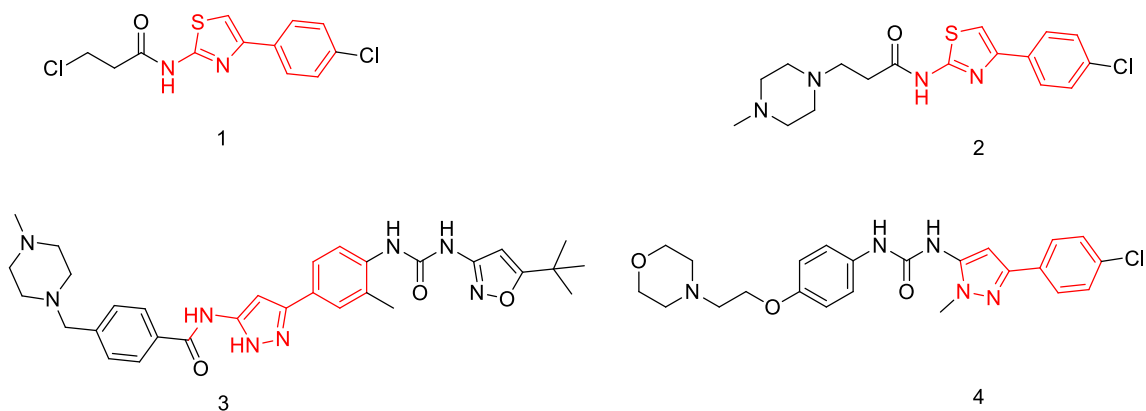


Fig. 1 Structures of known antineoplastic compounds 1–4

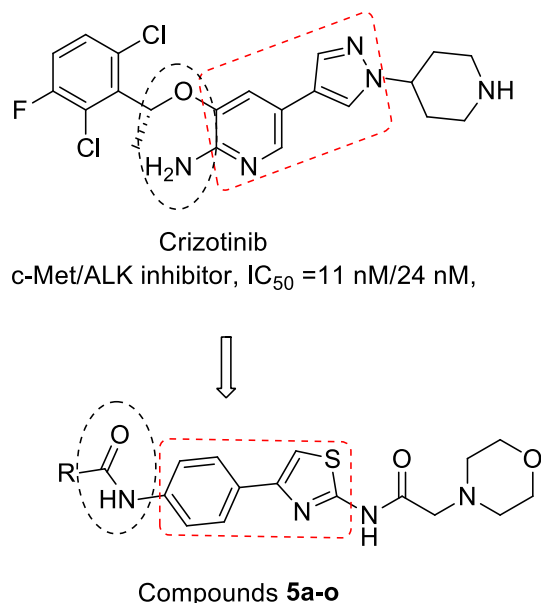


Fig. 2 The rational design of the novel target compounds

nitrogen atoms of morpholine ring can form the ionic form, similar to crizotinib (Cui et al. 2011; Huang et al. 2014; Shaw et al. 2016). We also employed an amide moiety instead of 2-amino and 3-alkoxy groups on the pyridine ring of crizotinib which contain a hydrogen bond donor–acceptor pair. To find a suitable replacement for the R group, various substituents on the phenyl ring and non-aromatic fragments were also included in the study. In this paper, we sought to develop novel 2,4-disubstituted thiazole amides with anti-proliferative activities. The general structure of the proposed targeted compounds is shown in Fig. 2.

## Experimental

### Chemicals, reagents and instruments

All reagents were purchased and used without further purification. Melting points were obtained in open capillaries using a WRS-1B melting point apparatus (Shen Guang, China) and were uncorrected. The  $^1\text{H}$  and  $^{13}\text{C}$  NMR spectra were recorded on a 400/54 Premium Shielded NMR Magnet System (Agilent, American). Mass spectral data were collected from an Agilent 6200 Series TOF and 6500 Series Q-TOF LC/MS System B.05.01. (B5125) in positive ion modes (Agilent, American). Analytical TLC was performed on silica gel 60 F254 plates (Merck, Germany).

### 4-(4-Nitrophenyl)thiazol-2-amine 1

A mixture of 2-bromo-1-(4-nitrophenyl) ethanone (2.44 g, 10.0 mmol) and thiourea (0.84 g, 10.0 mmol) was dissolved in anhydrous ethanol (20 mL). The reaction mixture was refluxed for 10 h. After confirmation of completion of the reaction by TLC, the reaction mixture was cooled to room temperature and then poured into cold water. It was then basified using saturated  $\text{NaHCO}_3$ . The resulting yellow solid was collected by suction filtration and washed with water. It was then dried to yield compound **1**.

Yellow solid; yield, 97.2%; m.p.: 273.4–274.6 °C;  $^1\text{H}$  NMR (400 MHz,  $\text{DMSO}-d_6$ )  $\delta$  8.28–8.19 (m, 2H), 8.09–8.00 (m, 2H), 7.42 (s, 1H), 7.26 (s, 2H);  $^{13}\text{C}$  NMR (101 MHz,  $\text{DMSO}-d_6$ )  $\delta$  169.0, 148.2, 146.3, 141.3, 126.7, 124.5, 107.0; HRMS ( $m/z$ ): calcd. for  $\text{C}_9\text{H}_8\text{N}_3\text{O}_2\text{S}$  (neutral  $\text{M}+\text{H}$ ) 222.03372, found 222.03352.

**2-Chloro-*N*-(4-(4-nitrophenyl)thiazol-2-yl)acetamide 2**

A solution of compound **1** (2.21 g, 10.0 mmol) and chloroacetic anhydride (3.42 g, 20.0 mmol) in acetonitrile (20 mL) was heated at 70 °C for 16 h. The reaction mixture was then concentrated and diluted with ethyl acetate. The organic layer was washed with a solution of sodium bicarbonate and water. The organics were combined, dried, filtered and the solvent removed under vacuum to yield compound **2**.

Yellow solid; yield, 84.1%; m.p.: 215.5–216.7 °C; <sup>1</sup>H NMR (400 MHz, Chloroform-*d*) δ 8.38–8.27 (m, 2H), 8.09–7.98 (m, 2H), 7.49–7.41 (m, 1H), 7.34–7.25 (m, 1H), 4.41–4.32 (m, 2H); <sup>13</sup>C NMR (101 MHz, Chloroform-*d*) δ 170.4, 159.1, 151.6, 148.0, 144.4, 126.6, 124.2, 111.9, 42.0; HRMS (*m/z*): calcd. For C<sub>11</sub>H<sub>9</sub>ClN<sub>3</sub>O<sub>3</sub>S (neutral M+H) 298.00531, found 298.00479.

**2-Morpholino-*N*-(4-(4-nitrophenyl)thiazol-2-yl)acetamide 3**

A mixture of compound **2** (2.97 g, 10.0 mmol), morpholine (0.96 g, 11.0 mmol), KI (0.17 g, 1.0 mmol) and anhydrous K<sub>2</sub>CO<sub>3</sub> (4.14 g, 30.0 mmol) in absolute ethanol (50 mL) was heated under reflux. After confirmation of completion of the reaction by TLC, the excess of ethanol was removed under vacuum and the residue extracted with CH<sub>2</sub>Cl<sub>2</sub>. The organic layer was washed with cold water, dried and the solvent removed under vacuum. The residue was crystallized from ethanol to give the product.

Yellow solid; yield, 88.2%; m.p.: 215.0–216.3 °C; <sup>1</sup>H NMR (400 MHz, chloroform-*d*) δ 10.36 (s, 1H), 8.29 (d, *J* = 8.7 Hz, 2H), 8.03 (d, *J* = 8.7 Hz, 2H), 7.40 (s, 1H), 3.85 (t, *J* = 4.6 Hz, 4H), 3.32 (s, 2H), 2.68 (t, *J* = 4.6 Hz, 4H); <sup>13</sup>C NMR (101 MHz, chloroform-*d*) δ 168.5, 157.5, 147.7, 147.1, 140.1, 126.6, 124.2, 111.5, 66.8, 61.4, 53.9; HRMS (*m/z*): calcd. For C<sub>15</sub>H<sub>17</sub>N<sub>4</sub>O<sub>4</sub>S (neutral M+H) 349.09705, found 349.09688.

***N*-(4-(4-aminophenyl)thiazol-2-yl)-2-morpholinoacetamide 4**

Compound **3** (0.35 g, 1.0 mmol) was dissolved in ethanol (20 mL) and SnCl<sub>2</sub>·2H<sub>2</sub>O (0.45 g, 2.0 mmol) was added. The mixture was refluxed for 4 h and ethanol was evaporated under vacuum. The residue was dissolved into CH<sub>2</sub>Cl<sub>2</sub> (40 mL) and then washed with dilute NaOH solution (1 mol/L, 3 × 20 mL) and water (3 × 20 mL), dried and evaporated to dryness to give the product.

Yellow solid; yield, 85.3%; m.p.: 181.5–182.8 °C; <sup>1</sup>H NMR (400 MHz, chloroform-*d*) δ 10.39 (s, 1H), 7.66 (d, *J* = 7.8 Hz, 2H), 6.97 (s, 1H), 6.74 (d, *J* = 7.8 Hz, 2H), 3.81 (d, *J* = 9.4 Hz, 4H), 3.26 (d, *J* = 3.8 Hz, 2H), 2.63 (s, 4H); <sup>13</sup>C NMR (101 MHz, chloroform-*d*) δ 168.2, 156.8, 150.3, 146.4, 127.2, 125.1, 115.1, 105.1, 66.8, 61.6, 53.9; HRMS

(*m/z*): calcd. For C<sub>15</sub>H<sub>19</sub>N<sub>4</sub>O<sub>2</sub>S (neutral M+H) 319.12287, found 319.12336.

**General procedure for the synthesis of compounds 5a-o**

To a mixture of compound **4** (32 mg, 0.1 mmol) and triethylamine (20 mg, 0.2 mmol) in CH<sub>2</sub>Cl<sub>2</sub> (20 mL), substituted acyl chloride (0.15 mmol) was added over a period of 10 min at 5 °C, and the reaction mixture was stirred at room temperature overnight. The reaction mixture was poured into H<sub>2</sub>O (500 mL) and extracted with CH<sub>2</sub>Cl<sub>2</sub>. The organic layer was washed with water, dried over anhydrous Na<sub>2</sub>SO<sub>4</sub> and concentrated under vacuum. The residual solid was purified by column chromatography on silica gel to give a target compound.

**3-Methyl-*N*-(4-(2-(2-morpholinoacetamido)thiazol-4-yl)phenyl)benzamide 5a**

Yellow solid; yield, 74.8%; m.p.: 197.0–198.9 °C; IR (KBr): *ν* 3043, 1873, 1852, 1770, 1750, 1479, 1345, 1265, 1238 cm<sup>-1</sup>; <sup>1</sup>H NMR (400 MHz, DMSO-*d*<sub>6</sub>) δ 12.09 (s, 1H), 10.33 (s, 1H), 7.95–7.84 (m, 4H), 7.79 (m, 2H), 7.58 (s, 1H), 7.44 (s, 2H), 3.64 (t, *J* = 4.5 Hz, 4H), 3.34 (s, 2H), 2.59–2.53 (m, 4H), 2.43 (s, 3H); <sup>13</sup>C NMR (101 MHz, DMSO-*d*<sub>6</sub>) δ 168.9, 166.1, 157.8, 149.1, 139.3, 138.2, 135.3, 132.6, 130.1, 128.8, 128.5, 126.4, 125.3, 120.7, 107.5, 66.6, 60.8, 53.4, 21.4; HRMS (*m/z*): calcd. For C<sub>23</sub>H<sub>25</sub>N<sub>4</sub>O<sub>3</sub>S (neutral M+H) 437.16474, found 437.17644.

**3,4-Dichloro-*N*-(4-(2-(2-morpholinoacetamido)thiazol-4-yl)phenyl)benzamide 5b**

Gray solid; yield, 77.0%; m.p.: 246.7–248.7 °C; IR (KBr): *ν* 3043, 1867, 1846, 1570, 1555, 1473, 1342, 1268, 1239 cm<sup>-1</sup>; <sup>1</sup>H NMR (400 MHz, DMSO-*d*<sub>6</sub>) δ 12.10 (s, 1H), 10.52 (s, 1H), 8.25 (d, *J* = 3.9 Hz, 1H), 7.94 (m, 3H), 7.86 (s, 2H), 7.86 (m, 1H), 7.60 (d, *J* = 4.0 Hz, 1H), 3.63 (d, *J* = 5.2 Hz, 4H), 3.34 (d, *J* = 4.0 Hz, 2H), 2.55 (d, *J* = 5.4 Hz, 4H); <sup>13</sup>C NMR (101 MHz, DMSO-*d*<sub>6</sub>) δ 168.9, 163.6, 157.8, 148.9, 138.8, 135.6, 134.8, 131.7, 131.2, 130.5, 130.0, 128.5, 126.5, 120.8, 107.7, 66.6, 60.8, 53.4; HRMS (*m/z*): calcd. For C<sub>22</sub>H<sub>21</sub>Cl<sub>2</sub>N<sub>4</sub>O<sub>3</sub>S (neutral M+H) 491.07114, found 491.07138.

**2,4-Dichloro-*N*-(4-(2-(2-morpholinoacetamido)thiazol-4-yl)phenyl)benzamide 5c**

Gray solid; yield, 79.1%; m.p.: 231.3–232.9 °C; IR (KBr): *ν* 3040, 1870, 1846, 1567, 1556, 1476, 1345, 1265, 1233 cm<sup>-1</sup>; <sup>1</sup>H NMR (400 MHz, DMSO-*d*<sub>6</sub>) δ 12.04 (s, 1H), 9.08 (s, 1H), 8.98 (s, 1H), 7.79 (d, *J* = 8.7 Hz, 2H), 7.54–7.45 (m, 5H), 7.14 (t, *J* = 1.9 Hz, 1H), 3.57 (t, *J* = 4.6 Hz, 4H), 3.27 (s, 2H), 2.49 (d, *J* = 4.5 Hz, 3H); <sup>13</sup>C NMR (101 MHz, DMSO-*d*<sub>6</sub>) δ 168.9, 164.4, 157.9, 148.9, 138.7, 136.1, 135.3, 131.6, 130.8, 130.4, 129.7, 127.9, 126.6, 120.1, 107.7, 66.6,

60.8, 55.4, 53.3; HRMS ( $m/z$ ): calcd. For  $C_{22}H_{21}Cl_2N_4O_3S$  (neutral  $M+H$ ) 491.07114, found 491.07255.

**3-Chloro-*N*-(4-(2-(2-morpholinoacetamido)thiazol-4-yl)phenyl)benzamide 5d** Yellow solid; yield, 74.0%; m.p.: 196.0–197.5 °C; IR (KBr):  $\nu$  3040, 1867, 1846, 1565, 1553, 1476, 1345, 1265, 1239  $cm^{-1}$ ;  $^1H$  NMR (400 MHz, DMSO- $d_6$ )  $\delta$  12.09 (s, 1H), 10.48 (s, 1H), 8.04 (d,  $J=1.9$  Hz, 1H), 7.99–7.83 (m, 5H), 7.70 (dd,  $J=7.9, 2.0$  Hz, 1H), 7.64–7.58 (m, 2H), 3.64 (t,  $J=4.6$  Hz, 4H), 3.34 (s, 2H), 2.55 (t,  $J=4.7$  Hz, 4H);  $^{13}C$  NMR (101 MHz, DMSO- $d_6$ )  $\delta$  168.9, 164.5, 157.8, 149.0, 138.9, 137.3, 133.6, 131.9, 130.9, 130.4, 127.8, 126.9, 126.5, 120.9, 107.7, 66.6, 60.8, 53.4; HRMS ( $m/z$ ): calcd. For  $C_{22}H_{22}ClN_4O_3S$  (neutral  $M+H$ ) 457.11011, found 457.11013.

**3-Bromo-*N*-(4-(2-(2-morpholinoacetamido)thiazol-4-yl)phenyl)benzamide 5e** Yellow solid; yield, 74.0%; m.p.: 196.0–197.5 °C; IR (KBr):  $\nu$  3042, 1869, 1852, 1565, 1555, 1476, 1342, 1265, 1237  $cm^{-1}$ ;  $^1H$  NMR (400 MHz, DMSO- $d_6$ )  $\delta$  12.06 (s, 1H), 10.42 (s, 1H), 8.12 (s, 1H), 7.95–7.90 (m, 1H), 7.90–7.74 (m, 5H), 7.54 (d,  $J=1.7$  Hz, 1H), 7.48 (t,  $J=7.9$  Hz, 1H), 3.58 (t,  $J=4.6$  Hz, 4H), 3.28 (s, 2H), 2.53–2.45 (m, 4H);  $^{13}C$  NMR (101 MHz, dmsO)  $\delta$  168.9, 164.4, 157.8, 149.0, 138.9, 137.5, 134.8, 131.1, 130.7, 130.4, 127.3, 126.5, 122.1, 120.8, 107.7, 66.6, 60.8, 53.4; HRMS ( $m/z$ ): calcd. For  $C_{22}H_{22}BrN_4O_3S$  (neutral  $M+H$ , neutral  $M+H+2$ ) 501.05960, found 501.067777, 503.06605.

**4-Bromo-*N*-(4-(2-(2-morpholinoacetamido)thiazol-4-yl)phenyl)benzamide 5f** Yellow solid; yield, 74.0%; m.p.: 191.1–193.0 °C; IR (KBr):  $\nu$  3046, 1870, 1849, 1565, 1547, 1473, 1345, 1256, 1238  $cm^{-1}$ ;  $^1H$  NMR (400 MHz, DMSO- $d_6$ )  $\delta$  12.06 (s, 1H), 10.39 (s, 1H), 7.92–7.78 (m, 6H), 7.76–7.71 (m, 2H), 7.54 (s, 1H), 3.57 (t,  $J=4.6$  Hz, 4H), 3.28 (s, 2H), 2.53–2.45 (m, 4H);  $^{13}C$  NMR (101 MHz, DMSO- $d_6$ )  $\delta$  168.9, 165.0, 157.8, 149.0, 139.0, 134.3, 131.9, 130.3, 130.2, 126.5, 125.8, 120.8, 107.6, 66.6, 60.8, 53.4; HRMS ( $m/z$ ): calcd. For  $C_{22}H_{22}BrN_4O_3S$  (neutral  $M+H$ ) 501.05960, found 501.067777, 503.06600.

**3-Fluoro-*N*-(4-(2-(2-morpholinoacetamido)thiazol-4-yl)phenyl)benzamide 5g** White solid; yield, 72.7%; m.p.: 200.1–201.9 °C; IR (KBr):  $\nu$  3040, 1867, 1846, 1567, 1558, 1479, 1351, 1274, 1239  $cm^{-1}$ ;  $^1H$  NMR (400 MHz, DMSO- $d_6$ )  $\delta$  12.08 (s, 1H), 10.44 (s, 1H), 7.92–7.79 (m, 6H), 7.61 (t,  $J=7.6$  Hz, 2H), 7.50 (d,  $J=9.6$  Hz, 1H), 3.64 (d,  $J=5.6$  Hz, 4H), 3.34 (d,  $J=4.1$  Hz, 2H), 2.70 (s, 4H);  $^{13}C$  NMR (101 MHz, DMSO- $d_6$ )  $\delta$  168.9, 164.6, 163.6, 161.1, 157.8, 149.0, 138.9, 137.6, 137.6, 131.1, 131.0, 130.4, 126.5, 124.3, 120.9, 119.1, 118.9, 115.0, 114.8, 107.7, 66.6, 60.8, 53.4; HRMS ( $m/z$ ): calcd.

For  $C_{22}H_{22}FN_4O_3S$  (neutral  $M+H$ ) 441.13966, found 441.14350.

**4-Fluoro-*N*-(4-(2-(2-morpholinoacetamido)thiazol-4-yl)phenyl)benzamide 5h** White solid; yield, 74.5%; m.p.: 205.6–206.8 °C; IR (KBr):  $\nu$  3043, 1869, 1846, 1570, 1550, 1476, 1348, 1268, 1239  $cm^{-1}$ ;  $^1H$  NMR (400 MHz, DMSO- $d_6$ )  $\delta$  12.12–12.07 (m, 1H), 10.40 (d,  $J=4.4$  Hz, 1H), 8.07 (d,  $J=6.7$  Hz, 2H), 7.96–7.83 (m, 4H), 7.62–7.56 (m, 1H), 7.41 (p,  $J=6.1$  Hz, 2H), 3.63 (d,  $J=5.7$  Hz, 4H), 3.36–3.30 (m, 2H), 2.71 (d,  $J=7.7$  Hz, 4H);  $^{13}C$  NMR (101 MHz, DMSO- $d_6$ )  $\delta$  168.9, 165.7, 164.9, 163.3, 157.8, 149.0, 139.1, 131.8, 131.7, 130.9, 130.8, 130.2, 126.4, 120.8, 115.9, 115.7, 107.6, 66.6, 60.8, 53.4; HRMS ( $m/z$ ): calcd. For  $C_{22}H_{22}FN_4O_3S$  (neutral  $M+H$ ) 441.13966, found 441.14684.

***N*-(4-(2-(2-Morpholinoacetamido)thiazol-4-yl)phenyl)-3-(trifluoromethyl)benzamide 5i** Gray solid; yield, 70.1%; m.p.: 210.08–211.9 °C; IR (KBr):  $\nu$  3043, 1870, 1846, 1567, 1553, 1476, 1345, 1271, 1239  $cm^{-1}$ ;  $^1H$  NMR (400 MHz, DMSO- $d_6$ )  $\delta$  12.09 (s, 1H), 10.60 (s, 1H), 8.31 (m, 2H), 8.01 (d,  $J=7.7$  Hz, 1H), 7.96–7.84 (m, 5H), 7.61 (s, 1H), 3.64 (d,  $J=5.6$  Hz, 4H), 3.34 (s, 2H), 2.56 (d,  $J=5.3$  Hz, 4H);  $^{13}C$  NMR (101 MHz, DMSO- $d_6$ )  $\delta$  168.9, 164.5, 157.8, 149.0, 138.8, 136.2, 132.3, 130.5, 130.2, 130.0, 129.8, 129.4, 128.6, 126.5, 125.8, 124.7, 124.6, 123.1, 121.0, 107.7, 66.6, 60.8, 53.4; HRMS ( $m/z$ ): calcd. For  $C_{23}H_{22}F_3N_4O_3S$  (neutral  $M+H$ ) 491.13647, found 491.13990.

***N*-(4-(2-(2-Morpholinoacetamido)thiazol-4-yl)phenyl)-4-(trifluoromethyl)benzamide 5j** Gray solid; yield, 72.2%; m.p.: 208.7–210.0 °C; IR (KBr):  $\nu$  3043, 1864, 1846, 1567, 1556, 1479, 1345, 1268, 1233  $cm^{-1}$ ;  $^1H$  NMR (400 MHz, DMSO- $d_6$ )  $\delta$  12.11 (s, 1H), 10.61 (s, 1H), 8.18 (d,  $J=8.1$  Hz, 2H), 7.99–7.85 (m, 6H), 7.61 (s, 1H), 3.64 (t,  $J=4.6$  Hz, 4H), 3.34 (s, 2H), 2.59–2.51 (m, 4H);  $^{13}C$  NMR (101 MHz, DMSO- $d_6$ )  $\delta$  168.9, 164.8, 157.8, 149.0, 139.1, 138.9, 132.0, 131.6, 130.5, 129.0, 128.7, 126.5, 125.9, 125.9, 125.9, 125.8, 125.7, 123.0, 120.9, 107.7, 66.6, 60.8, 53.4; HRMS ( $m/z$ ): calcd. For  $C_{23}H_{22}F_3N_4O_3S$  (neutral  $M+H$ ) 491.13647, found 491.13719.

***N*-(4-(2-(2-morpholinoacetamido)thiazol-4-yl)phenyl) furan-2-carboxamide 5k** White solid; yield, 86.6%; m.p.: 190.1–192.2 °C; IR (KBr):  $\nu$  3046, 1870, 1849, 1566, 1550, 1479, 1342, 1250  $cm^{-1}$ ;  $^1H$  NMR (400 MHz, DMSO- $d_6$ )  $\delta$  12.03 (s, 1H), 10.27 (s, 1H), 7.91 (d,  $J=1.6$  Hz, 1H), 7.87–7.74 (m, 4H), 7.52 (s, 1H), 7.32 (d,  $J=3.4$  Hz, 1H), 6.68 (dd,  $J=3.5, 1.8$  Hz, 1H), 3.57 (t,  $J=4.6$  Hz, 4H), 3.27 (s, 2H), 2.50–2.47 (m, 4H);  $^{13}C$  NMR (101 MHz, DMSO- $d_6$ )  $\delta$  168.9, 157.8, 156.6, 149.0, 147.8, 146.3,

138.6, 130.2, 126.5, 120.8, 115.3, 112.7, 107.6, 66.6, 60.8, 53.4; HRMS ( $m/z$ ): calcd. For  $C_{20}H_{21}N_4O_4S$  (neutral  $M+H$ ) 413.12835, found 413.12688.

**2-Methoxy-*N*-(4-(2-(2-morpholinoacetamido)thiazol-4-yl)phenyl)acetamide 5l** White solid; yield, 79.5%; m.p.: 149.4–190.7 °C; IR (KBr):  $\nu$  3040, 1867, 1846, 1570, 1556, 1476, 1339, 1271, 1235  $cm^{-1}$ ;  $^1H$  NMR (400 MHz, DMSO- $d_6$ )  $\delta$  12.10 (s, 1H), 9.89 (s, 1H), 7.86 (d,  $J=8.5$  Hz, 2H), 7.76 (d,  $J=8.5$  Hz, 2H), 7.56 (s, 1H), 4.04 (s, 2H), 3.63 (t,  $J=4.6$  Hz, 4H), 3.40 (s, 3H), 3.33 (s, 2H), 2.56–2.53 (m, 4H);  $^{13}C$  NMR (101 MHz, DMSO- $d_6$ )  $\delta$  168.9, 168.5, 157.8, 149.0, 138.5, 130.0, 126.5, 120.2, 107.5, 72.1, 66.6, 60.8, 59.1, 53.4; HRMS ( $m/z$ ): calcd. For  $C_{18}H_{23}N_4O_4S$  (neutral  $M+H$ ) 391.14400, found 391.14442.

***N*-(4-(2-(2-Morpholinoacetamido)thiazol-4-yl)phenyl)cyclohexanecarboxamide 5m** White solid; yield, 71.8%; m.p.: 158.9–160.1 °C; IR (KBr):  $\nu$  3037, 1867, 1849, 1570, 1553, 1479, 1348, 1265, 1242  $cm^{-1}$ ;  $^1H$  NMR (400 MHz, DMSO- $d_6$ )  $\delta$  12.01 (s, 1H), 9.89 (s, 1H), 7.77 (d,  $J=8.7$  Hz, 2H), 7.62 (d,  $J=8.7$  Hz, 2H), 7.47 (s, 1H), 3.57 (t,  $J=4.6$  Hz, 4H), 3.26 (s, 2H), 2.52–2.43 (m, 4H), 2.29 (m, 1H), 1.80–1.55 (m, 6H), 1.44–1.30 (m, 2H), 1.29–1.09 (m, 2H);  $^{13}C$  NMR (101 MHz, DMSO- $d_6$ )  $\delta$  174.8, 168.9, 157.7, 149.1, 139.5, 129.4, 126.5, 119.5, 107.2, 66.5, 60.8, 53.4, 45.3, 29.6, 25.8, 25.7; HRMS ( $m/z$ ): calcd. For  $C_{22}H_{29}N_4O_3S$  (neutral  $M+H$ ) 429.19604, found 429.20332.

***N*-(4-(4-Acetamidophenyl)thiazol-2-yl)-2-morpholinoacetamide 5n** White solid; yield, 93.6%; m.p.: 202.3–204.0 °C; IR (KBr):  $\nu$  3043, 1870, 1849, 1567, 1553, 1475, 1342, 1265, 1230  $cm^{-1}$ ;  $^1H$  NMR (400 MHz, DMSO- $d_6$ )  $\delta$  12.04 (s, 1H), 10.01 (s, 1H), 7.82–7.75 (m, 2H), 7.60 (d,  $J=8.5$  Hz, 2H), 7.47 (s, 1H), 3.57 (t,  $J=4.6$  Hz, 4H), 3.27 (s, 2H), 2.49–2.47 (m, 4H), 2.02 (s, 3H);  $^{13}C$  NMR (101 MHz, DMSO- $d_6$ )  $\delta$  168.9, 168.8, 157.8, 149.1, 139.4, 129.5, 126.5, 119.4, 107.2, 66.6, 60.8, 55.4, 53.4, 24.5; HRMS ( $m/z$ ): calcd. For  $C_{17}H_{21}N_4O_3S$  (neutral  $M+H$ ) 361.13344, found 361.13904.

**2-Chloro-*N*-(4-(2-(2-morpholinoacetamido)thiazol-4-yl)phenyl)acetamide 5o** White solid; yield, 86.8%; m.p.: 205.8–208.0 °C; IR (KBr):  $\nu$  3040, 1867, 1849, 1570, 1550, 1479, 1342, 1271, 1244  $cm^{-1}$ ;  $^1H$  NMR (400 MHz, DMSO- $d_6$ )  $\delta$  12.09 (s, 1H), 10.41 (s, 1H), 7.87–7.79 (m, 2H), 7.66–7.59 (m, 2H), 7.52 (s, 1H), 4.24 (s, 2H), 3.58 (t,  $J=4.5$  Hz, 4H), 3.31 (s, 2H), 2.52 (s, 4H);  $^{13}C$  NMR (101 MHz, DMSO- $d_6$ )  $\delta$  165.1, 157.8, 148.9, 138.5, 130.3, 126.7, 119.8, 107.7, 66.4, 60.6, 55.4, 53.3, 44.0; HRMS ( $m/z$ ): calcd. For  $C_{17}H_{20}ClN_4O_3S$  (neutral  $M+H$ ) 395.09446, found 395.09553.

## Anticancer assay

The antiproliferative activity of the target compounds on the human non-small cell lung cancer cell (A549), human cervical cancer cell (Hela), human colon cancer cell (HT29) and human lymphoma cell line (Karpas299) was tested using the MTT assay. A549, HeLa and HT29 cell lines were obtained from the Cell Resource Center (Shanghai Institutes for Biological Sciences, China Academy of Sciences). Karpas299 cell line was purchased from Nanjing Cobioer Biosciences Company. The cells were seeded in 96-well microplates at a density of  $5 \times 10^3$  cells per well and incubated with 5%  $CO_2$  at 37 °C. On the next day, the target compounds were added into the culture medium at a five times concentration gradient. The final concentration of DMSO in the medium was less than 0.5%. Triplicates of each concentration were used. After 48 h incubation, the supernatant was removed and 5 mg/mL of a freshly prepared solution of MTT was added to each well. The plates were then incubated with the cells at 37 °C for another 4 h. The medium was removed and 100  $\mu$ L of DMSO was added to each well to dissolve the formazan. The microplate reader was used to measure the absorbance at 490 nm (for absorbance of MTT formazan) and 630 nm (for the reference wavelength). Cell growth inhibition rates formula is  $(AC - AT)/AC \times 100\%$  ( $AC$ , absorbance value of the blank control group;  $AT$ , absorbance value of the experimental group). The  $IC_{50}$  was calculated using GraphPad Prism version 6.00 software from the non-linear curve.

## Western blot

HT29 cells were treated with the compounds for 2 h at 37 °C, followed by being lysed in RIPA buffer (150 mM NaCl, 1% NP-40, 1% SDS, 1 mM PMSF, 10  $\mu$ g/ml leupeptin, 1 mM aprotinin, 50 mM Tris-Cl, pH 7.4) for 30 min. The protein concentration was determined by the BCA assay. Cell lysates (50  $\mu$ g each lane) were separated by 10% SDS-PAGE and then transferred to PVDF membrane. The membrane was blocked with 5% non-fat milk for 1 h, incubated with 1:1000 diluted primary antibodies for 3 h and stained with 1:2000 diluted HRP-conjugated secondary antibodies for 30 min at room temperature. Bound antibodies were revealed by enhanced chemiluminescence (ECL).

## Molecular docking

The molecular docking procedure was performed by using a CDocker algorithm for receptor–ligand interactions of Accelrys Discovery Studio. The crystal structure of c-Met kinase (PDB code 2WGJ) and ligand was prepared as described previously (Li et al. 2018). The parameters were

used to accomplish this task with default values. The lowest energy docked complex was the optimal docking conformation of the target compound.

## Results and discussion

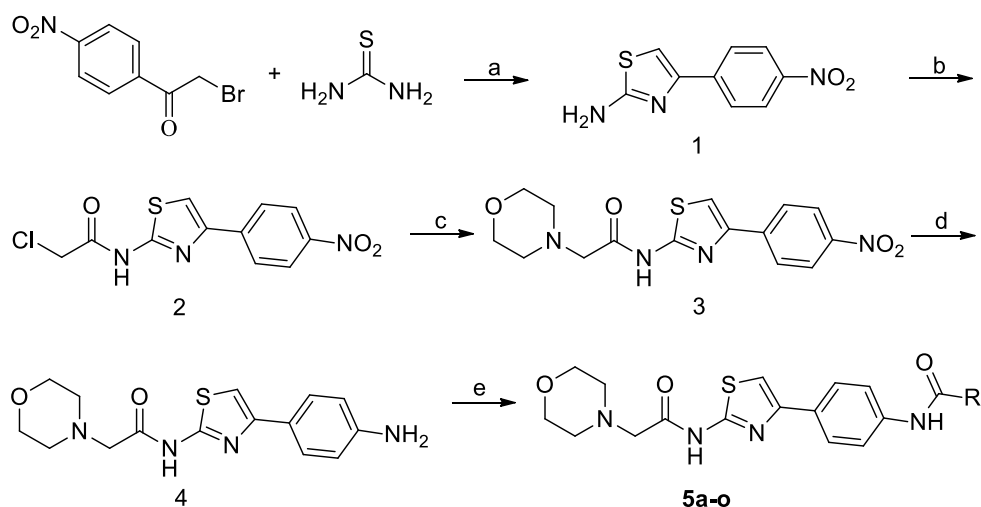
### Chemistry

The 2-aminothiazole amide derivatives **5a–o** were synthesized by the general procedure shown in Scheme 1. The compound **1** was prepared in good yields by the modified

Hantzsch thiazole condensation of 2-bromo-1-(4-nitrophenyl)ethanone with thiourea in refluxing ethanol. Heating of the aminothiazole **1** with the excess chloroacetic anhydride in acetonitrile generated compound **2**. Compound **3** was obtained by the alkylation reaction between compound **2** and morpholine. Reduction with tin (II) chloride dihydrate in refluxing ethanol yielded compound **4**. The target compounds **5a–o** were prepared by coupling aromatic amine **4** with the appropriate acyl chloride by using dichloromethane as a solvent in the presence of triethylamine.

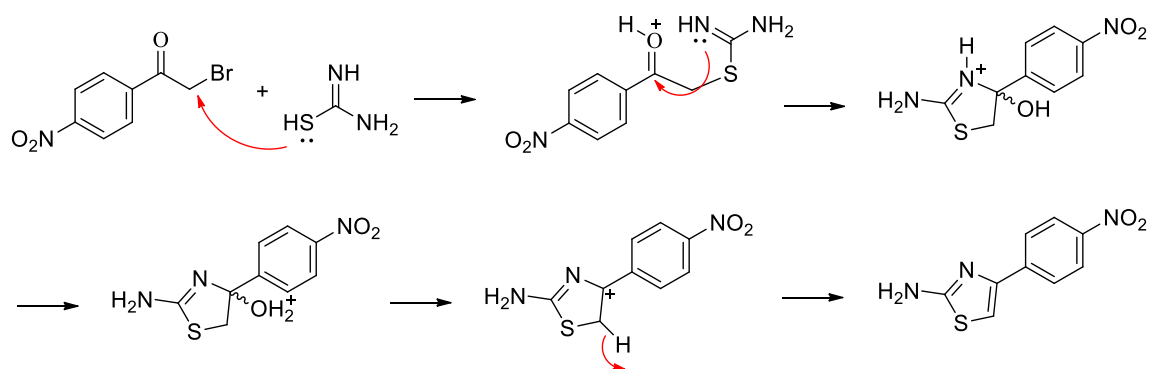
The mechanisms of compound **1** formation can be explained as follows (Scheme 2): Thiourea undergoes

**Scheme 1** Synthesis of the target compounds



Comp	R	Comp	R	Comp	R
5a		5b		5c	
5d		5e		5f	
5g		5h		5i	
5j		5k		5l	
5m		5n		5o	

Reagents and conditions: (a) *thiourea*, ethanol, reflux; (b) chloroacetic anhydride, acetonitrile, 70 °C; (c) morpholine, ethanol, Na<sub>2</sub>CO<sub>3</sub>, r.t.; (d) SnCl<sub>2</sub>·2H<sub>2</sub>O, ethanol, reflux; (e) substituted acyl chloride, CH<sub>2</sub>Cl<sub>2</sub>, Et<sub>3</sub>N, r.t.



**Scheme 2** The possible mechanisms of 2-aminothiazole derivatives formation

**Table 1** IC<sub>50</sub> (μM) of the target compounds

Comp.	A549	Hela	HT29	Karpas299
<b>5a</b>	> 40	> 40	> 40	> 40
<b>5b</b>	8.46	6.05	0.63	13.87
<b>5c</b>	21.30	18.69	10.11	14.27
<b>5d</b>	13.24	8.81	6.33	17.45
<b>5e</b>	18.83	17.25	14.15	34.52
<b>5f</b>	24.08	20.68	18.63	> 40
<b>5g</b>	14.66	13.75	10.36	28.06
<b>5h</b>	20.52	16.35	13.46	30.44
<b>5i</b>	> 40	> 40	> 40	> 40
<b>5j</b>	> 40	> 40	> 40	> 40
<b>5k</b>	> 40	33.51	17.66	> 40
<b>5l</b>	> 40	> 40	> 40	> 40
<b>5m</b>	> 40	> 40	> 40	> 40
<b>5n</b>	> 40	> 40	> 40	> 40
<b>5o</b>	> 40	> 40	> 40	> 40
Crizotinib	2.39	1.10	1.09	0.03

tautomerism and the sulfur atom of isothioureia tautomeric form may be more susceptible to nucleophilic attack (Devarajan et al. 1993; Morales-Bonilla et al. 2006). The sulfur atom uses one of its lone pair of electrons to form a single bond to the saturated carbon of the α-halogen ketone. Subsequently, carbonyl carbon is condensed with an enamine fragment to yield cyclic intermediate catalyzed by HBr generated in situ. Finally, the dehydration process results in a cation intermediate, which leads to 2-aminothiazole.

## Biological activity and discussion

All the target compounds were assayed for cell proliferation inhibition using MTT assay with four tumor cell lines, including the A549, HeLa, HT29 and Karpas299 cell lines. Crizotinib was used as a positive control. The biological data are summarized in Table 1.

The results of an MTT assay showed that some target compounds significantly inhibited the growth of HT29 colon cancer cells (c-Met overexpression). However, most of the target compounds did not substantially inhibit the proliferation of the Karpas299 cells (ALK overexpression).

To investigate whether the cellular activity can be improved, the substituent R of the target compounds was altered. Compound **5a** in comparison with **5d**, **5e**, **5g** showed that the meta-halogen-substituted phenyl ring was more efficient than the meta-methyl-substituted phenyl ring in terms of cellular activities. Compounds **5d**, **5e**, **5g** with the meta-halogen at the phenyl ring all possessed better antitumor activity. These results demonstrated that the introduction of a meta-halogen (especially chloro)-substituted phenyl ring at R significantly influenced the activity. Comparing the compounds with different chloro-substitution positions on the phenyl ring, their activity order was m-Cl > 3,4-Cl<sub>2</sub> > 2,4-Cl<sub>2</sub> and their activities suggest that ortho-chloro-substituted phenyl rings at R are unfavorable. The compounds **5i** and **5j** were completely inactive on cells. This observation suggests that a moderate polar group on the phenyl ring at R is detrimental to anticancer activities. The activity of compound **5k**, in which the phenyl ring at R is replaced by a furan ring fragment, is worse than that of compound **5b**. In contrast, the alkyl group was introduced instead of the phenyl ring at R, showing even worse activities toward the test cells. This suggests that target compounds possessing aromatic moieties of the R position may have played an important role in increasing antiproliferative properties.

## Molecular properties and drug likeness

Estimation of drug-likeness properties has been used as tools to reduce attrition in the process of oral drug discovery and development. All compounds **10a–j** were calculated online using the free molecular calculation services provided by MolSoft (<http://molsoft.com/mprop>), as shown in Table 2.

**Table 2** Molecular properties and drug-likeness

Comp.	MW	HBA	HBD	MolLogP	MolPSA	Score
<b>5a</b>	436.16	6	2	3.36	67.89	0.94
<b>5b</b>	490.06	6	2	4.27	67.89	1.03
<b>5c</b>	490.06	6	2	4.27	67.89	1.19
<b>5d</b>	456.10	6	2	3.67	67.89	1.11
<b>5e</b>	500.05	6	2	3.81	67.89	0.88
<b>5f</b>	500.05	6	2	3.81	67.89	1.17
<b>5g</b>	440.13	6	2	3.23	67.89	1.04
<b>5h</b>	440.13	6	2	3.23	67.89	1.33
<b>5i</b>	490.13	6	2	4.20	67.89	0.83
<b>5j</b>	490.13	6	2	4.20	67.89	0.79
<b>5k</b>	412.12	7	2	2.19	76.47	1.18
<b>5l</b>	390.14	7	2	1.12	76.38	1.22
<b>5m</b>	428.19	6	2	3.16	68.09	1.08
<b>5n</b>	360.13	6	2	1.52	68.07	1.11
<b>5o</b>	394.09	6	2	1.74	67.95	1.03
Crizotinib	449.12	4	3	3.95	62.56	0.36
Desirable value	< 500	< 10	< 5	< 5	< 140	

MW molecular weight, HBA number of hydrogen bond acceptors, HBD number of hydrogen bond donors, MolLogP LogP value predicted by MolSoft, MolPSA topological polar surface area, Å<sup>2</sup>, Score molecular drug-likeness model score, Desirable value acceptable molecular properties

For most target compounds, the drug-likeness properties such as MW, HBA, HBD, MolLogP and MolPSA were all in the range of the desirable values. Only the MW value of compounds **5e** and **5f** were slightly higher than the desirable value. Thus, it is conceivable that these compounds might have ideal drug-likeness properties. The drug-likeness model score were calculated and possessed a positive score from 0.83 to 1.22 (Table 2), which implied these compounds to be good drug candidates. In some cases, lipophilicity seemed to have an important influence on their antiproliferative activities. The compounds **5b–h** possessed an appropriate MolLogP value in the range of 3.23–4.27, which was very close to the value of crizotinib. This result was in accordance with the better anticancer activities of compounds **5b–h**. However, compounds **5i** and **5j** endowed with high MolLogP values showed reduced activity, probably due to strong electron-withdrawing effect exerted by trifluoromethyl groups.

### Western blot analysis

Given the inhibitory activity of target compounds on cancer cell lines, we further tested whether the compounds could inhibit the proliferation and growth by inhibiting MET signaling in c-Met altered cancers. Compound **5b** and **5f** were selected for further experiment. As shown in Fig. 3, crizotinib (5 μM) obviously inhibited the phosphorylation of c-Met in HT29 cells, and **5b** (5 μM) also significantly decreased the levels of c-Met phosphorylation in HT29 cells. These results demonstrate that the target compound,

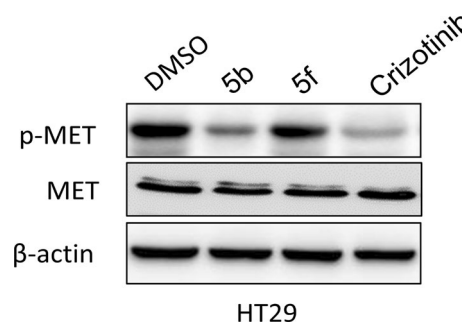


**Fig. 3** Effect of crizotinib and the target compounds on c-MET expression in HT29 cancer cell

especially for compound **5b**, could be used to block the MET signaling pathway.

### Docking study

To better understand the receptor–ligand interactions, molecular docking was performed between the crystal structure of c-Met kinase (PDB code 2WGJ) and small molecules (crizotinib and compound **5b**) using a CDocker protocol of Accelrys Discovery Studio. Docking accuracy was assessed by redocking crizotinib from complexes. The root-mean-square deviation (RMSD) between the optimal docking conformation and the ligand geometry from X-ray of the complex reached 0.6807 Å, which implied that the docking method provided reliable bioactive conformations. The 3D

docking results (Fig. 4) showed similar binding modes of crizotinib and compound **5b** within the unphosphorylated c-Met kinase (2WGJ) domain. These docking results indicated that these two ligands probably have similar pharmacological properties.

For crizotinib (Fig. 5a), the two hydrogen bonds were formed between the 2-aminopyridyl group and the Met1160, Pro1158, respectively. Other notable interactions include a  $\pi$ - $\pi$  interaction between the 3-(1*H*-pyrazol-4-yl)pyridine core and Tyr1230. The hydrophobic interaction with the enzyme, such as Met1211 and Gly1163, may be intensified at the U-shaped binding site.

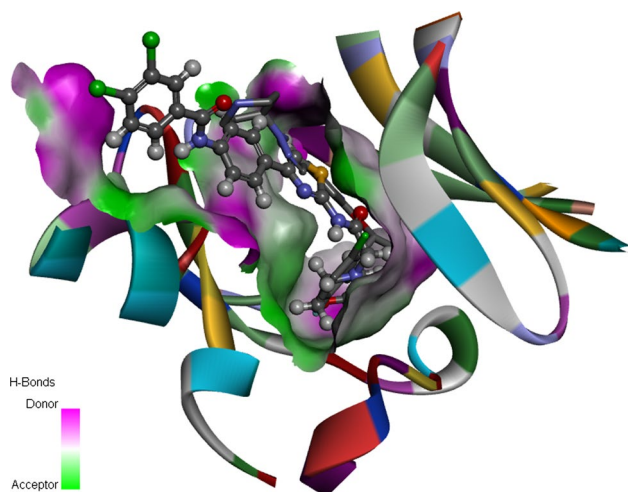


**Fig. 4** Poses of crizotinib (stick) and compound **5b** (ball and stick) in the active site of c-Met kinase

ATP-competitive, small-molecule inhibitors of the c-Met kinase usually interact with the residue Met1160 via hydrogen bond at the hinge region (Parikh and Ghatge 2017). The optimal docking conformation of the compound **5b** was located in a nearly identical position to that mentioned above (Fig. 5b). In the binding mode, compound **5b** was well embedded in the crizotinib binding pocket. The 2-morpholinoacetamido fragment formed a hydrogen bond with Asp1164 and the thiazole ring formed a  $\pi$ - $\pi$  interaction with Met1160. But unexpectedly, the 2-morpholinoacetamido fragment of compound **5b** and the substituted phenyl group of crizotinib were found to occupy a similar position. The 3D diagrams showed that the morpholine ring in the side chain of compound **5b** did not interact with the residue Tyr1230 of the activation loop through typical  $\pi$ - $\pi$  interaction. Compound **5b** adopted an extended conformation, which resulted in weak interaction between the ligand and the enzyme, and thus decreased the bioactivity. From these observations, it is possible that modifying the 2-morpholinoacetamido fragment can contribute to improving the bioactivity of these target compounds.

## Conclusions

We have designed and synthesized a novel series of 2,4-disubstituted thiazole amide derivatives, according to the structural characteristics of c-Met inhibitors crizotinib. Some of these compounds exhibited medium or better in vitro anti-proliferative activity against A549, Hela, HT29 and Karpas299 cells. The western blot analysis and molecular docking study supported the development of 2,4-disubstituted

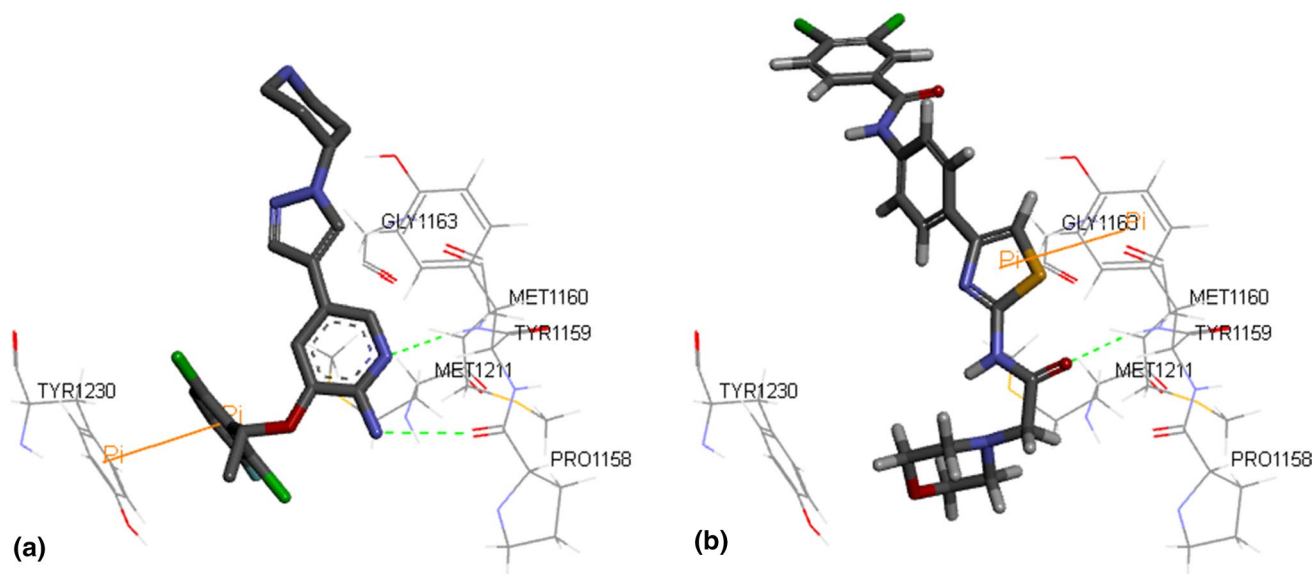


**Fig. 5** **a** Crizotinib in a complex with a c-Met protein (active site). **b** A docked conformation of compound **5b** in a c-Met binding site

thiazole amide-based compounds as potential c-Met inhibitors.

**Acknowledgements** This work was supported by the National Natural Science Foundation of China (No. 21601075), the Natural Science Foundation of Liaoning Province (Nos. 2015020249, 20170540396) and General Research Projects of Liaoning Provincial Department of Education (No. JQL201715410).

## References

- Alam MS, Liu L, Lee YE, Lee DU (2011) Synthesis, antibacterial activity and quantum-chemical studies of novel 2-arylidenehydrazinyl-4-arylthiazole analogues. *Chem Pharm Bull (Tokyo)* 59:568–573. <https://doi.org/10.1248/cpb.59.568>
- Bhat S, Shim JS, Liu JO (2013) Tricyclic thiazoles are a new class of angiogenesis inhibitors. *Bioorg Med Chem Lett* 23:2733–2737. <https://doi.org/10.1016/j.bmcl.2013.02.067>
- Chang HH, Song Z, Wisner L, Tripp T, Gokhale V, Meuillet EJ (2012) Identification of a novel class of anti-inflammatory compounds with anti-tumor activity in colorectal and lung cancers. *Invest New Drugs* 30:1865–1877. <https://doi.org/10.1007/s10637-011-9748-8>
- Cui JJ, Trandubé M, Shen H, Nambu M, Kung PP, Pairish M, Jia L, Meng J, Funk L, Botrous I (2011) Structure based drug design of crizotinib (PF-02341066), a potent and selective dual inhibitor of mesenchymal-epithelial transition factor (c-MET) kinase and anaplastic lymphoma kinase (ALK). *J Med Chem* 54:6342–6363. <https://doi.org/10.1021/jm2007613>
- Devarajan R, Arunachalam V, Jayakumar E, Selvi P (1993) Water-soluble polymers. I. Synthesis of *N*-succinimido (*N*) thiocarbonyl acrylamide and its polymerization: grafting of this monomer and acrylamide onto poly (vinyl alcohol). *J Appl Polym Sci* 48:921–930. <https://doi.org/10.1002/app.1993.070480516>
- El-Messery SM, Hassan GS, Al-Omary FA, El-Subbagh HI (2012) Substituted thiazoles VI. Synthesis and antitumor activity of new 2-acetamido- and 2 or 3-propanamido-thiazole analogs. *Eur J Med Chem* 54:615–625. <https://doi.org/10.1016/j.ejmech.2012.06.013>
- Gennäs GB, Mologni L, Ahmed S, Rajaratnam M, Marin O, Lindholm N, Viltadi M, Gambacorti-Passerini C, Scapozza L, Yli-Kauhaluoma J (2011) Design, synthesis, and biological activity of urea derivatives as anaplastic lymphoma kinase inhibitors. *ChemMedChem* 6:1680–1692. <https://doi.org/10.1002/cmdc.201100168>
- Hassan GS, El-Messery SM, Al-Omary FAM, El-Subbagh HI (2012) Substituted thiazoles VII. Synthesis and antitumor activity of certain 2-(substituted amino)-4-phenyl-1,3-thiazole analogs. *Bioorg Med Chem Lett* 22:6318–6323. <https://doi.org/10.1016/j.bmcl.2012.08.095>
- Huang Q, Johnson TW, Bailey S, Brooun A, Bunker KD, Burke BJ, Collins MR, Cook AS, Cui JJ, Dack KN, Deal JG, Deng Y-L, Dinh D, Engstrom LD, He M, Hoffman J, Hoffman RL, Johnson PS, Kania RS, Lam H, Lam JL, Le PT, Li Q, Lingardo L, Liu W, Lu MW, McTigue M, Palmer CL, Richardson PF, Sach NW, Shen H, Smeal T, Smith GL, Stewart AE, Timofeevski S, Tsaparikos K, Wang H, Zhu H, Zhu J, Zou HY, Edwards MP (2014) Design of potent and selective inhibitors to overcome clinical anaplastic lymphoma kinase mutations resistant to crizotinib. *J Med Chem* 57:1170–1187. <https://doi.org/10.1021/jm401805h>
- Li J, Zheng T-C, Jin Y, Xu J-G, Yu J-G, Lv Y-W (2018) Synthesis, molecular docking and biological evaluation of quinolone derivatives as novel anticancer agents. *Chem Pharm Bull* 66:55–60. <https://doi.org/10.1248/cpb.c17-00035>
- Morales-Bonilla P, Pérez-Cardena A, Quintero-Mármol E, Arias-Téllez JL, Mena-Rejón GJ (2006) Preparation, antimicrobial activity, and toxicity of 2-amino-4-arylthiazole derivatives. *Heteroat Chem* 17:254–260. <https://doi.org/10.1002/hc.20182>
- Parikh PK, Ghate MD (2017) Recent advances in the discovery of small molecule c-Met Kinase inhibitors. *Eur J Med Chem* 143:1103–1138. <https://doi.org/10.1016/j.ejmech.2017.08.044>
- Shaw AT, Friboulet L, Leshchiner I, Gainor JF, Bergqvist S, Brooun A, Burke BJ, Deng Y-L, Liu W, Dardaei L, Frias RL, Schultz KR, Logan J, James LP, Smeal T, Timofeevski S, Katayama R, Iafrate AJ, Le L, McTigue M, Getz G, Johnson TW, Engelman JA (2016) Resensitization to crizotinib by the lorlatinib ALK resistance mutation L1198F. *New Engl J Med* 374:54–61. <https://doi.org/10.1056/NEJMoa1508887>
- Siddiqui HL, Zia-Ur-Rehman M, Ahmad N, Weaver GW, Lucas PD (2007) Synthesis and antibacterial activity of bis[2-amino-4-phenyl-5-thiazolyl] disulfides. *Chem Pharm Bull (Tokyo)* 55:1014–1017. <https://doi.org/10.1248/cpb.55.1014>
- Smith B, Chang HH, Medda F, Gokhale V, Dietrich J, Davis A, Meuillet EJ, Hulme C (2012) Synthesis and biological activity of 2-aminothiazoles as novel inhibitors of PGE2 production in cells. *Bioorg Med Chem Lett* 22:3567. <https://doi.org/10.1016/j.bmcl.2012.03.013>
- Solomon B (2014) Refining the toxicity profile of Crizotinib. *J Thorac Oncol* 9:1596–1597. <https://doi.org/10.1097/JTO.0000000000000375>
- Tu C-H, Lin W-H, Peng Y-H, Hsu T, Wu J-S, Chang C-Y, Lu C-T, Lyu P-C, Shih C, Jiaang W-T, Wu S-Y (2016) Pyrazolylamine derivatives reveal the conformational switching between type i and type ii binding modes of anaplastic lymphoma kinase (ALK). *J Med Chem* 59:3906–3919. <https://doi.org/10.1021/acs.jmedchem.6b00106>
- Wilson TR, Fridlyand J, Yan Y, Penuel E, Burton L, Chan E, Peng J, Lin E, Wang Y, Sosman J (2014) Widespread potential for growth-factor-driven resistance to anticancer kinase inhibitors. *Nature* 487:505–509. <https://doi.org/10.1038/nature11249>
- Zhou L, Yang Q, Wang Y, Hu Y, Luo X, Bai D, Li S (2008) Synthesis and biological evaluation of novel isopropanolamine derivatives as non-peptide human immunodeficiency virus protease inhibitors. *Chem Pharm Bull (Tokyo)* 56:1147–1152. <https://doi.org/10.1248/cpb.56.1147>